Pulse collapse and blue-shifted enhanced supercontinuum in a photonic crystal fiber*

Liu Wen-Jun(刘文军)†, Pang Li-Hui(庞利辉), Lin Xiang(林 翔), Gao Ren-Xi(高仁喜), and Song Xiao-Wei(宋晓伟)

Department of Optoelectronics Science, Harbin Institute of Technology at Weihai, Weihai 264209, *China*

(Received 23 July 2012; revised manuscript received 30 September 2012)

The blue-shifted supercontinuum generation in a photonic crystal fiber pumped by high peak power femtosecond pulses with a wavelength located in the anomalous dispersion region is investigated experimentally and numerically. The formation of a blue-shifted enhanced supercontinuum due to the pulse collapse is demonstrated. The process of the pulse collapse is measured by using the grating-eliminated no-nonsense observation of ultrafast incident laser light e-fields technique (GRENOUILLE). Numerical simulations in spectral and temporal domains are conducted. The data from the numerical simulations are in good agreement with the experimental results. Our experimental results and numerical simulations show that pulse collapse is the determining factor in the generation of a blue-shifted supercontinuum.

Keywords: femtosecond pulse, ultrafast measurement, supercontinuum

PACS: 42.65.–k, 42.65.Jx, 42.65.Tg **DOI:** 10.1088/1674-1056/22/3/034204

1. Introduction

The structure of photonic crystal fiber (PCF) provides a wavelength-dependent effective index for the cladding and allows the single-mode guidance throughout the visible and the near infrared spectral ranges. This leads to novel features in nonlinear processes, such as the generation of a supercontinuum (SC) with a spectral width exceeding two octaves for relatively low intensities and long pulses. The SC generation depends on the pulse duration, the pulse energy, and the pump wavelength in relation to the zero-dispersion wavelength. Extensive studies reveal that several physical phenomena are involved in the process of supercontinuum generation. Self-phase modulation, intrapulse Raman scattering, four-wave mixing, cross-phase modulation, modulation instability, and dispersive wave generation are the major nonlinear processes that actively take part in supercontinuum generation.[1–4]

The interplay between the dispersion and the nonlinearity of the PCF produces optical solitons whose dynamics play a pivotal role in the process of supercontinuum generation when an ultrashort optical pulse is launched in the anomalous group-velocity dispersion domain. In this case, the spectral broadening is governed by the transformation of the pump pulse into higher-order solitons that break up through the effects of higher-order dispersion and Raman scattering. The resulting fundamental solitons shift to lower frequencies via the soliton self-frequency shift.[5–9] Since the magnitude of the soliton self-frequency shift inversely increases with the increasing pulse duration, the soliton self-frequency shift of the solitons created after fission leads to a red spectral broadening in the PCF with anomalous group velocity dispersion.[10–14] At the same time, the dispersive wave generation extends the spectrum into the visible and the ultraviolet spectral ranges where the group velocity dispersion is normal.

Many theoretical studies on supercontinuum generation in a PCF pumped by femtosecond pulses at relatively low input energies are carried out, but experimental studies on the temporal evolution of the pulse in a PCF are relatively rare due to the fiber diffraction and the measuring difficulty. Dudley and Cao simulated and measured the continuum generations in a 16-cm PCF and a 8-mm PCF, respectively using XFROG.[15,16] However, XFROG is not suitable to measure a weak signal due to its complex structure.

The SC generation process is very complex, and the rich dynamic evolution is certainly not apparent by simply measuring the spectrum at the fiber output. Its practical applications require that we understand how best to create it. Finding the answer requires detailed modeling and wholly measuring the SC. In this paper, we present experimental and numerical results on the SC generation in a PCF, and the pump wavelength is located in the anomalous dispersion regime. To investigate the temporal and the spectral evolutions of femtosecond pulses in the PCF, the grating-eliminated no-nonsense observation of ultrafast incident laser light e-fields (GRENOUILLE) technique is used in experiments. GRENOUILLE is a simple and compact method for measuring complex ultrashort pulses. It requires only a few simple optical elements and no intricate alignment procedure. In addition, it can measure pulses from

*Project supported by the National Natural Science Foundation of China (Grant No. 61178025), the Natural Science Foundation of Shandong Province, China (Grant Nos. ZR2009AL002 and ZR2010FQ007), and the Natural Scientific Research Innovation Foundation in Harbin Institute of Technology, China (Grant No. HIT.NSRIF. 2008087).

†Corresponding author. E-mail: liuwenjun86@163.com

© 2013 Chinese Physical Society and IOP Publishing Ltd

a wide variety of sources, from the lowest-energy oscillator to the highest-intensity amplifier. The GRENOUILLE is also extremely compact and more sensitive than other pulse diagnostics. GRENOUILLE's operating range nicely matches that of most ultrafast Ti:Sapphire lasers and amplifiers.[17]

We study the spectral broadening dynamics into the blue and the red spectral ranges as functions of the input power. We find that the underlying broadening mechanism on the blue side depends strongly on the input power whereas that on the red side does not. We simulate its evolution in the spectral and temporal domains to clarify the underlying physics. The data from numerical simulations are in good agreement with the experimental results. At a high pulse energy and in the anomalous dispersion regime, the pump pulse evolves toward a high-order soliton. Because of the higher-order dispersion, the high-order soliton is not stable and breaks up into constituent solitons, resulting in the emission of blue-shifted non-solitonic radiation. Our experimental and simulation results show that the pulse collapse plays a crucial role in the blue-shifted supercontinuum generation.

2. Experimental setup

Figure 1 shows a diagram of the experimental setup. The pulse duration is $T_{\mathrm{FWHM}} = 120$ fs with a central wavelength of 800 nm. The bandwidth of the pulse is about 10 nm, and the pulse repetition rate is 1 kHz. The energy is controlled by an attenuator. The laser beam is focused into the PCF by a 10× microscope objective. The fiber output is recorded using an optical spectrometer, and a home made GRENOUILLE is used to measure the temporal evolution of the pulse.

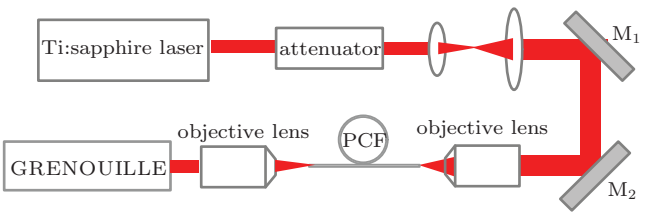


Fig. 1. (color online) Diagram of experimental setup.

The supercontinuum generation is studied in a 10 cm long PCF. The dispersion of the fiber is shown in Fig. 2(a), and a scanning electron micrograph of the fiber cross-section is shown in Fig. 2(b). The diameter of the solid core of the fiber is 2.5 μm, the diameter of the hole is 2.7 μm with hole-to-hole spacing of 2.9 μm. The zero-dispersion wavelength is located at 780 nm; the nonlinear parameter is $\sim 0.09\ \mathrm{W^{-1}\cdot m^{-1}}$.

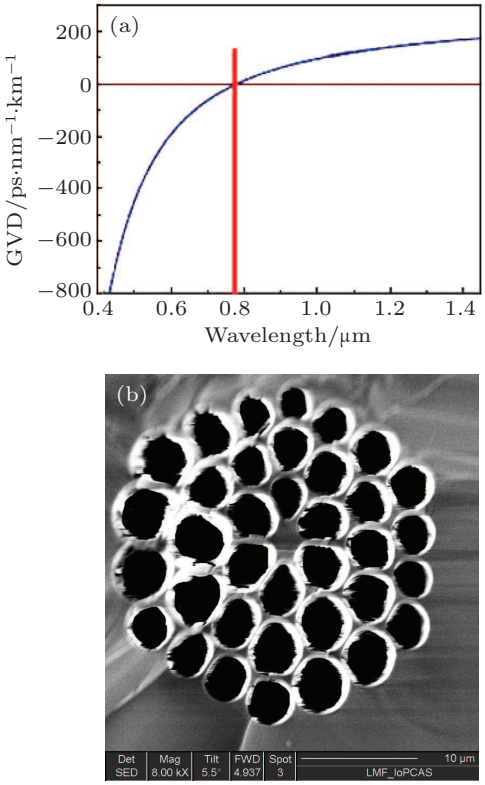


Fig. 2. (color online) (a) Dispersion of the fiber as a function of wavelength, (b) scanning electron micrograph of the fiber transverse section.

3. Results and discussion

Figure 3(a) is a photograph of the beam propagating in the PCF. The laser beam is focused into the PCF at the left entrance surface by a 10× microscope objective, and the beam in the PCF propagates from left to right. The output pattern at the exit surface of the PCF is imaged on a CCD camera as shown in Fig. 3(b). A blue-shifted SC is generated in the PCF, as the color shown in the photograph is blue-shifted, and the blue-shifted SC generation is confirmed in Fig. 4.



Fig. 3. (color online) (a) Photograph of blue-shifted SC; (b) output pattern of the fiber.

The output spectra recorded for different input powers are presented in Fig. 4. The distinctive features of the output spectra are the spectral evolution being highly asymmetric around the zero dispersion wavelength and the appearance of blue-shifted enhanced frequency components. In Fig. 4(a), the input power is 20 mW, and the spectrum shows a broadened pump along with two features. The first feature is at the long wavelength side of the pump pulse, where a part of the energy is transferred to several distinct peaks with central wavelengths of 830 nm, 845 nm, 880 nm, and 965 nm. The second feature in the spectrum is that the blue-shifted components are

simultaneously generated and a gap is formed in the vicinity of the zero-dispersion wavelength 780 nm. The distinct peaks of the blue-shifted components are located at 774 nm, 555 nm, and 500 nm. A further increase in the power leads to a continuous blue-shift to 350 nm, and more blue-shift peaks appear. At higher pump energies, all these peaks merge to give a continuous spectrum. With a further increase in the power, the intensity of the blue band grows and the edge of the spectrum shifts to a shorter wavelength, whereas the red side of the spectrum is found to expand rather moderately, as shown in Figs. 4(b)–4(d). The transmitted spectra are attenuated by an attenuator and recorded by a USB2000+ Miniature fiber optic spectrometer.

The solitons in the spectral domain in Figs. 4(b)–4(d) cannot be discerned due to the spectral overlap of the solitons with increasing pump intensity. Solitons in the temporal domain with a different lag time measured by the GRENOUILLE are illustrated in Fig. 6.

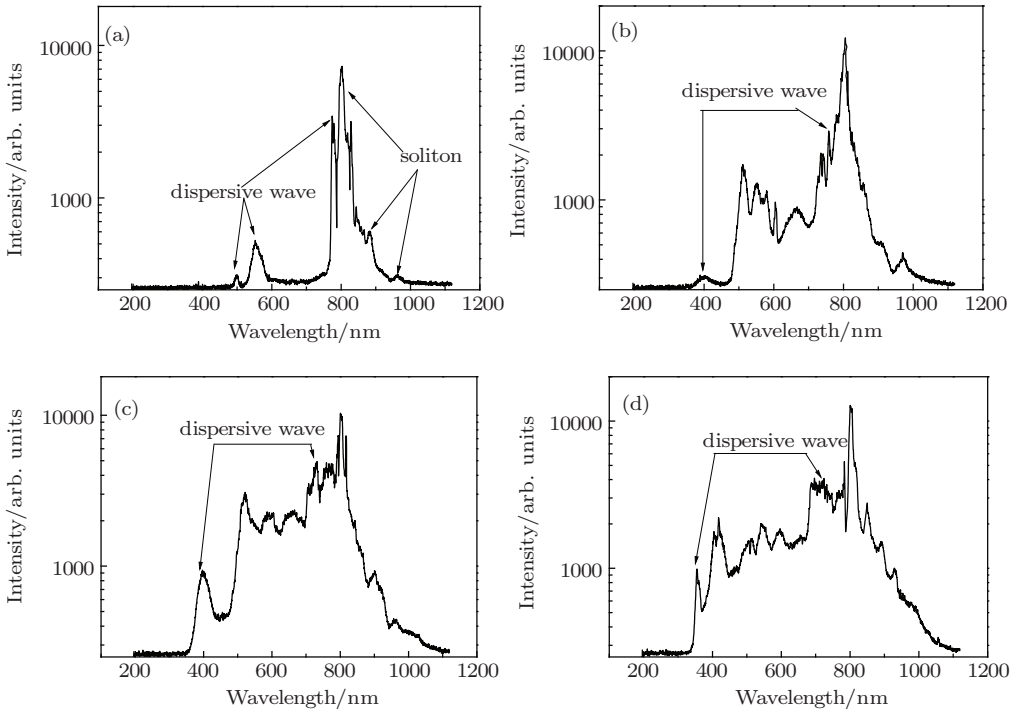


Fig. 4. Output spectra recorded for for different input powers ((a) 20 mW, (b) 25 mW, (c) 30 mW, (d) 35 mW).

The behavior of SC generation in the fiber described above cannot be explained only by the self-phase modulation induced broadening. We can explain the appearance of this series of new spectral peaks in terms of the fission of higher-order solitons.[18] At high pulse energy and with a pump wavelength in the anomalous dispersion regime, the pump pulse evolves toward a high-order soliton. The red-shifted new peaks are the result of soliton fission in the fiber. Because the pump pulse is launched in the anomalous dispersion domain and is near the zero dispersion wavelength, a high-order soliton is not stable and breaks up into constituent first-order solitons due to the contributions from other effects such as self-steepening, high-order dispersion, and Raman scattering. The initial pulse collapses into sub-pulses with different group velocities, different widths, and different peak powers, which appear in the optical spectrum as the red-shifted components. The blue-shifted components originate in the fission process, a part of the pulse energy is transferred to a dispersive wave at the frequency that satisfies a specific phase-matching condition, and it falls on the blue side of the original carrier frequency of the incident pulse.[21] The phase-matching conditions for resonant dispersive wave generation can be used for the optimization of wavelength conversion into blue and ultraviolet spectral ranges.[19]

In order to study the temporal evolution of the input pulse, we construct a GRENOUILLE setup to measure the temporal evolution of the pulses. Figure 5 shows a series of experimental traces measured for different input power levels. The retrieved supercontinuum intensity and phase vs. time for different input powers are shown in Fig. 6. The supercontinuum in the temporal domain consists of a series of sub-pulses that are much shorter than the input 120 fs pulse. In particular, the figure shows the temporal pulse collapse and the development of ultrafast temporal oscillations on portions of the temporal intensity profile. The temporal characteristics shown in Fig. 6 are in good agreement with the above analysis. The initial pulse collapses into sub-pulses with different group velocities, different widths, and different peak powers, which separate

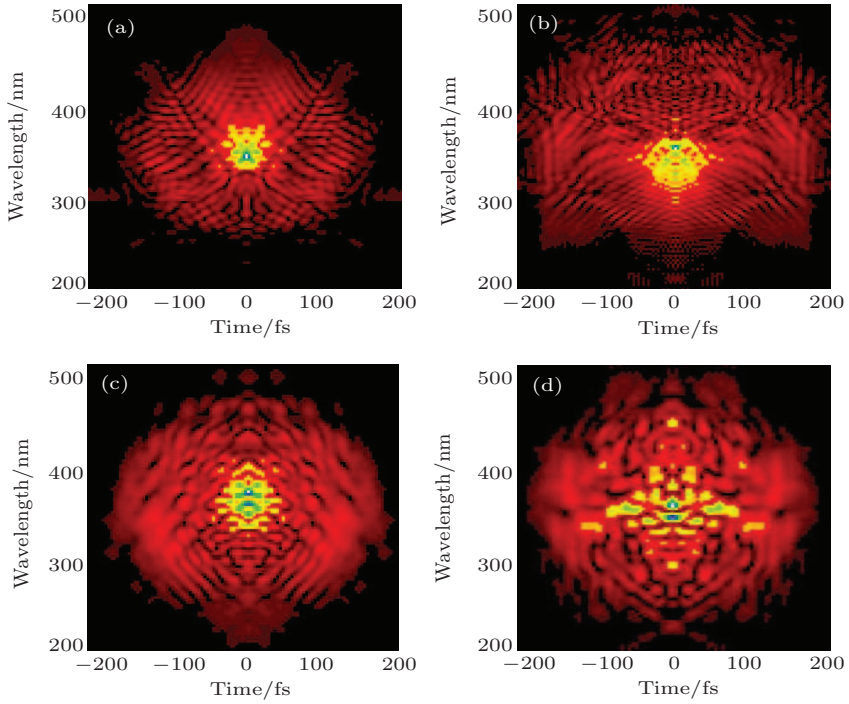


Fig. 5. (color online) Experimental traces in the PCF measured for different input powers ((a) 20 mW, (b) 25 mW, (c) 30 mW, (d) 35 mW).

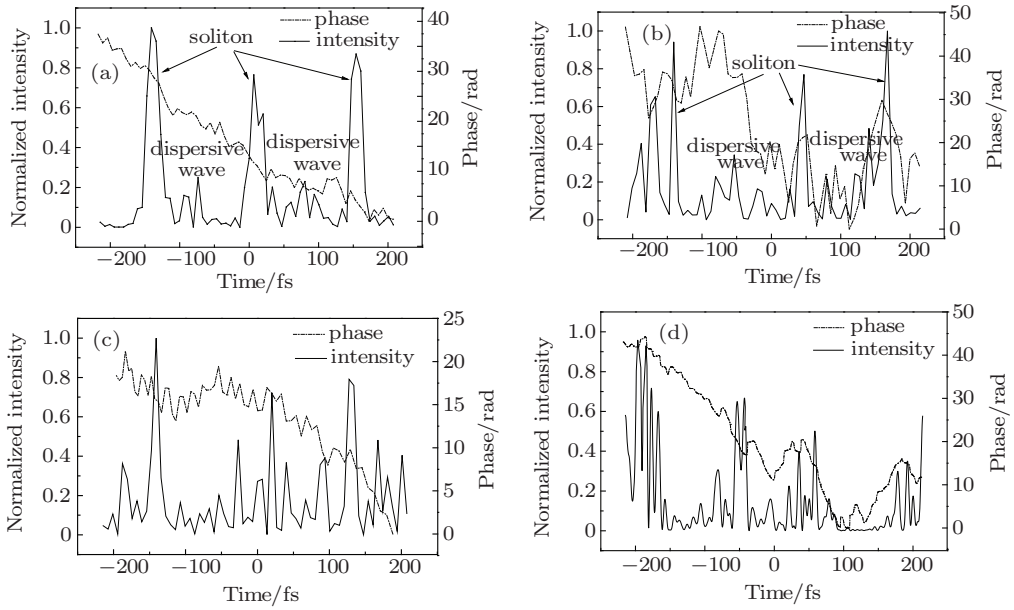


Fig. 6. Retrieved supercontinuum intensity and phase versus time in the PCF for different input powers ((a) 20 mW, (b) 25 mW, (c) 30 mW, (d) 35 mW).

from each other due to the group velocity walk-off. The pulse launched into the fiber corresponds to an N-th order soliton. Such a soliton is constituted of N fundamental solitons. The number of these fundamental solitons increases with increasing input pulse energy, as shown in Fig. 6.

4. Numerical simulation

The generalized nonlinear Schrödinger equation (GNLSE) is widely used to simulate the dynamics of SC generation and can be written in the normalized form as[1,20]

$$\frac{\partial A}{\partial z}+\frac{\alpha}{2}A=\mathrm{i}\sum_{m=1}^{\infty}\frac{\mathrm{i}^m\beta_m}{m!}\frac{\partial^m A}{\partial t^m}+\mathrm{i}\gamma\left(1+\frac{\mathrm{i}}{\omega_0}\frac{\partial}{\partial t}\right)\times\left(A(z,t)\int_0^{\infty}R(t')\left|A(z,t-t')\right|^2\mathrm{d}t'\right), \quad (1)$$

where α accounts for the fiber losses, and γ is the nonlinear parameter. By assuming that the electronic contribution is nearly instantaneous, $R(t)$ can be written as

$$R(t)=(1-f_{\mathrm{R}})\delta(t)+f_{\mathrm{R}}h_{\mathrm{R}}(t), \quad (2)$$

where $f_R = 0.245$, and the first and the second terms correspond to the electronic and the Raman responses, respectively. The Raman response function can be expressed in the form

$$h_R(\tau) = (f_a + f_c)h_a(\tau) + f_b h_b(\tau), \tag{3}$$

where functions $h_a(\tau)$ and $h_b(\tau)$ are defined as

$$h_a(\tau) = \frac{\tau_1^2 + \tau_2^2}{\tau_1 \tau_2^2} \exp\left(-\frac{\tau}{\tau_2}\right) \sin\left(\frac{\tau}{\tau_1}\right), \tag{4}$$

$$h_b(\tau) = \left(\frac{2\tau_b - \tau}{\tau_b^2}\right) \exp\left(-\frac{\tau}{\tau_b}\right), \tag{5}$$

with $\tau_1 = 12$ fs, $\tau_2 = 32$ fs, and $\tau_b = 96$ fs. The coefficients

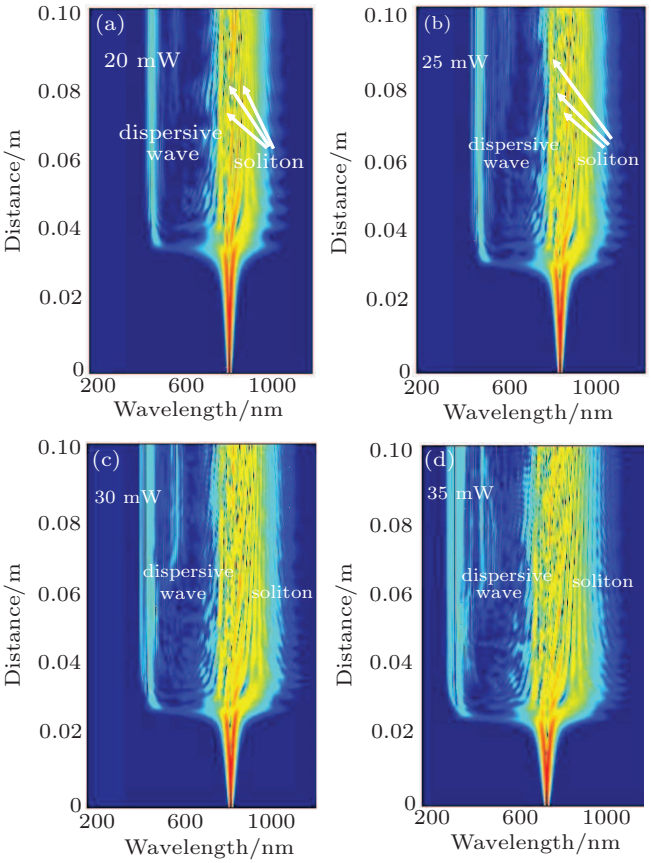


Fig. 7. (color online) Simulated spectral evolutions of the pulse in the PCF for different input powers ((a) 20 mW, (b) 25 mW, (c) 30 mW, (d) 35 mW).

$f_a = 0.75$, $f_b = 0.21$, and $f_c = 0.04$ quantify the relative contributions of the isotropic and the anisotropic parts of the Raman response. The standard split-step Fourier method is employed to solve the GNLSE numerically. The input pulse is assumed to have a Gaussian shape with pulse width $T_0 = 120$ fs. The other parameters are $\lambda_0 = 802$ nm, $\alpha = 0$, $\gamma = 0.09$ W^{-1}·m^{-1}, $\beta_2 = -5 \times 10^{-26}$ s^2/m, $\beta_3 = 1.4 \times 10^{-40}$ s^3/m, and the propagation distance is 0.1 m.

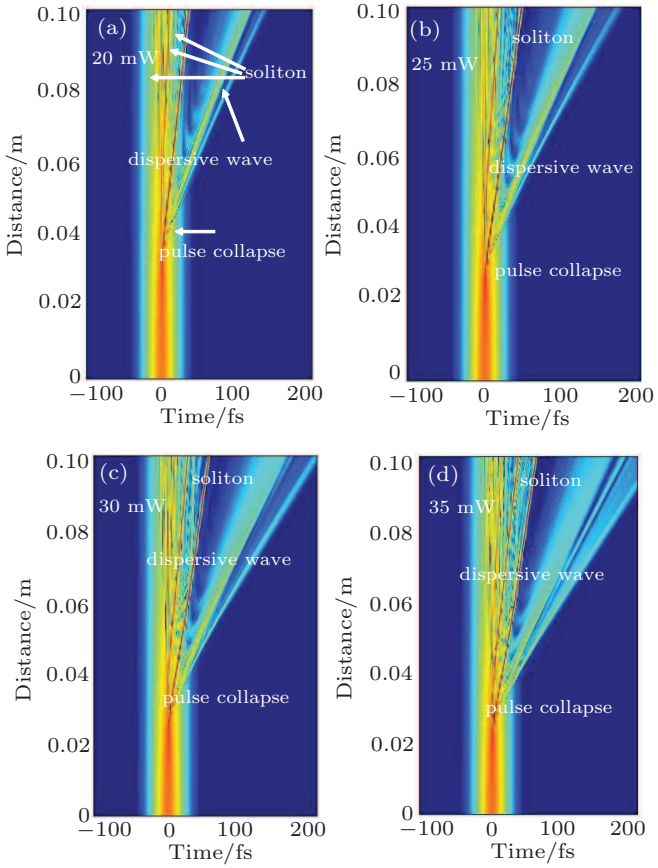


Fig. 8. (color online) Simulated temporal evolutions of the pulse in the PCF for different input powers ((a) 20 mW, (b) 25 mW, (c) 30 mW, (d) 35 mW).

The simulated spectral evolutions of the input pulses in the PCF with different input powers are plotted in Fig. 7. As can be seen from Fig. 7, the supercontinuum is significantly blue-shifted. New spectral frequencies are generated first on both sides of the input frequency due to the self-phase modulation. These self-phase modulation induced components broaden the spectrum over its input width. In Fig. 7(a), the input power is 20 mW, the distinct peak of the blue-shifted component is located approximately at 500 nm, and the red side of the spectrum is expanded simultaneously. With increasing input power, more blue-shifted peaks are generated and the intensity of the blue band grows, whereas the red side of the spectrum is found to expand rather moderately. As the input power reaches 35 mW, the blue-shifted spectrum approaches nearly 200 nm. The simulated spectra coincide with the experimental results. An optical soliton is generated by the low-frequency components of the spectrum; however, some of the pulse energy lies in the blue part falling in the normal group velocity dispersion domain, as shown in Fig. 7.

The simulated temporal evolutions of the input pulses with different input powers are plotted in Fig. 8. As shown in Fig. 8, the input pulse narrows in the first few centimeters of the fiber due to the self-phase modulation and the anomalous dispersion, and later, in conjunction with the high-order dispersion terms and other disturbing effects, the pulse col-

lapses. This is the process referred to as the soliton fission. Solitons are shed one after another and shift to a longer wavelength as expected from the soliton self-frequency shift. The solitons separate in the temporal domain due to the group velocity walk-off. At the same time, we can see that the soliton is delayed more and more as it propagates, and its spectrum shifts towards the red side. As can be seen from Fig. 8, as the soliton is further red-shifted, a part of the dispersive wave shifts toward the blue side as shown in Fig. 7. The dispersive wave moves slower than the soliton and appears behind the soliton during the propagation.

The dispersion length of the fiber for the pulse width of $T_0 = 120$ fs is $L_D = 0.288$ m, and the nonlinear length for the pulse peak power of $P_0 = 2\times10^8$ W is $L_{\rm NL} = 0.06$ μm. These input parameters imply that the input pulse can be treated as a higher-order soliton. The pulse launched into the fiber corresponds to an N-th order soliton. The N-th order soliton collapses and the initial pulse decays into sub-pulses which propagate independently as fundamental solitons. The sub-pulses are far less stable than the fundamental solitons. As the pump power increases, the sub-pulses shed away energy, then they can propagate as the fundamental solitons, and the radiated energy transfers to a dispersive wave and falls on the blue side. The extension of the continuum to the infrared is not significant; consequently, the Raman scattering is not the determining factor in our experiments. The delay of sub-pulses which behave like the fundamental solitons is a result of the lower velocities of the frequency components that form them. The number of these fundamental solitons increases with the increase in input pulse energy. The input pulses initially undergo the expected higher-order soliton evolution dynamics of spectral broadening and temporal compression; however, because of perturbations such as the higher-order dispersion and the stimulated Raman scattering, the dynamics depart from the recurrent behavior expected for the ideal high-order solitons, and the pulses collapse.[21,22] When close to the zero-dispersion wavelength, however, such an idealized soliton fission does not occur in practice, because the same perturbations that induce the breakup in the first place also modify the subsequent evolution of the ejected solitons. In the initial stage, for example, the energy of the ejected solitons is shed via the generation of dispersive wave spectral components in the normal dispersion regime, whilst continued propagation leads to a continuous shift to longer wavelengths through the Raman soliton self-frequency shift, and the cross-phase modulation between the Raman-shifting solitons and the dispersive waves.[20]

5. Conclusion

In this paper, we have investigated the blue-shifted supercontinuum generation in a PCF pumped by high peak power femtosecond pulses with a pulse width of 120 fs and wavelength in the anomalous dispersion regime of the PCF. The formation of a blue-shifted enhanced supercontinuum due to pulse collapse is demonstrated. The process of the pulse collapse is measured by using the GRENOUILLE. The data from numerical simulations are in good agreement with the experimental results. The results show that increasing the pump power leads to a broadening in the blue-shifted components, whereas the red side of the spectrum is found to expand rather moderately. The process creates blue-shifted new frequency components that ultimately form the supercontinuum. The spectrum is mainly generated by the soliton fission and the dispersive wave generation. The initial pulse starts to collapse into sub-pulses, causing the central part of the spectrum to be broadened. The sub-pulses shed away energy so the pulses can propagate as independent fundamental solitons; the radiated energy is in the spectrum as blue-shifted components. The soliton self-frequency shift of the single solitons created after fission leads to red spectral broadening in the fiber with anomalous dispersion. The dispersive wave generation extends the spectrum into the visible and the ultraviolet spectral ranges where the dispersion is normal. The spectral and the temporal profiles of the pulse suffer strongly from the high-order dispersion and other disturbing effects, resulting in asymmetric spectral broadening (more broadened on the blue side).

References

[1] Agrawal G P 2007 *Nonlinear Fiber Optics* (4th edn.) (San Diego: Academic Press)
[2] Genty G, Lehtonen M and Ludvigsen H 2004 *Opt. Express* **12** 4614
[3] Genty G, Dudley J M and Eggleton B J 2009 *Appl. Phys. B* **94** 187
[4] Song R, Hou J, Chen S P, Yang W Q and Lu Q S 2012 *Chin. Phys. B* **21** 094211
[5] Tai K, Hasegawa A and Bekki N 1988 *Opt. Lett.* **13** 392
[6] Beaud P, Hodel W, Zysset B and Weber H P 1987 *IEEE Journal of Quantum Electronics* **23** 1938
[7] Kodama Y and Hasegawa A 1987 *IEEE Journal of Quantum Electronics* **23** 510
[8] Mitschke F M and Mollenauer L F 1986 *Opt. Lett.* **11** 659
[9] Chen W, Meng Z and Zhou H J 2012 *Chin. Phys. B* **21** 094215
[10] Herrmann J and Nazarkin A 1994 *Opt. Lett.* **19** 2065
[11] Herrmann J, Griebner U, Zhavoronkov N, Husakou A, Nickel D, Knight J C, Wadsworth W J, Russell J and Korn G 2002 *Phys. Rev. Lett.* **88** 173901
[12] Jin A J, Wang Z F, Hou J, Guo L and Jiang Z F 2012 *Acta Phys. Sin.* **61** 124211 (in Chinese)
[13] Gross B and Manassah J T 1992 *J. Opt. Soc. Am. B* **9** 1813
[14] Hilligsøe K M and Paulsen H N 2003 *J. Opt. Soc. Am. B* **20** 1887
[15] Dudley J, Gu X, Xu L, Kimmel M, Zeek E, O'Shea P, Trebino R, Coen S and Windeler R 2002 *Opt. Express* **10** 1215
[16] Cao Q, Gu X, Zeek E, Kimmel M, Trebino R, Dudley and Windeler R S 2003 *Appl. Phys. B* **77** 239
[17] Trebino R, Bowlan P, Gabolde P, Gu X, Akturk S and Kimmel M 2009 *Laser & Photon. Rev.* **3** 314
[18] Husakou A V and Herrmann J 2001 *Phys. Rev. Lett.* **87** 203901
[19] Karpman V I 1993 *Phys. Rev. E* **47** 2073
[20] Dudley J M and Taylor J R 2010 *Supercontinuum Generation in Optical Fibers* (Cambridge: Cambridge University Press)
[21] Dianov E M, Karasik A Y, Mamyshev P V, Prokhorov A M, Serkin V N, Stelmakh M F and Fomichev A A 1985 *JETP Lett.* **41** 294
[22] Golovchenko E A, Dianov E M, Prokhorov A M and Serkin V N 1985 *JETP Lett.* **42** 74